

PRODUCTION OF STOPPED PIONS AND MUONS FROM A

MULTI-BEV PROTON SYNCHROTRON *

V.W. Hughes and R.D. Edge †

Gibbs Laboratory, Yale University

Summary

The use of a multi-BeV synchrotron as a high intensity source of stopped pions and muons is discussed. To produce stopped pions extraction of pions at a relatively low energy between 100 and 200 MeV is necessary due to pion absorption in the attenuator used to stop the pions. Although no experimental data appear to be available on the cross section for production of such low energy pions by multi-BeV protons, we can use experimental data on the production of higher energy pions together with an empirical formula for the pion energy spectrum to estimate that the production cross section for 200 MeV positive or negative pions by 30 BeV protons is about 50 $\mu\text{b}/\text{sr}/\text{MeV}/\text{Be}^9$ nucleus at a laboratory angle of 5° . Using such a cross section and considering other relevant factors we conclude that the proton linac accelerator meson factory operating at 500 MeV with 6×10^{15} protons/sec will produce about 100 times as many stopped pions or muons as could be obtained in practice from the Brookhaven National Laboratory Alternating Gradient Synchrotron operating with an increased intensity of 2×10^{13} protons/sec.

1. Introduction

The possibility of using a multi-BeV proton synchrotron - for example, the 30 BeV Alternating Gradient Synchrotron at the Brookhaven National Laboratory - as a useful source of stopped pions and stopped muons is considered. Such a possibility is of considerable interest because if the high energy synchrotron were a useful, high intensity source of stopped pions and muons, then it could serve as an alternative for this purpose to a lower energy, high intensity proton accelerator - a so-called "meson factory." This matter has been discussed so far primarily in the unpublished literature.^{1,2,3}

The factors that must be considered in determining the density of stopped pions are given in the following equation.

* Research supported in part by the U.S. Atomic Energy Commission.
 † Present address: Physics Department, University of South Carolina

$$\frac{dn_\pi}{dR} = IN \Delta \Omega \frac{d^2 \sigma}{d\Omega dT} f_D f_A \frac{dT}{dR} \quad (1)$$

in which dn_π/dR = number of pions stopping per unit time(sec) and per unit range (gm/cm^2); I = incident proton beam intensity in protons/sec; N = number of target atoms/ cm^2 ; $\Delta \Omega$ = solid angle for pion collection in sr; $(d^2 \sigma/d\Omega dT)$ is the differential cross section for pion production per unit solid angle and per MeV interval of kinetic energy, T ; f_D = fraction of pions which survive decay; f_A = fraction of pions which do not undergo an attenuating collision in the absorber or the proton target. This equation does not take into account straggling due to multiple Coulomb scattering. For determining the density of stopped muons a similar equation applies with the addition of factors to account for the probability that a pion decays into a muon with a particular kinetic energy T_μ and that this muon is captured in the beam transport system.⁴

2. Pion Production Cross Sections

Because the attenuation of high energy pions by the absorber is very large (f_A small) and also because the lateral spread due to multiple Coulomb scattering is large (See section 3), stopped pions are produced most advantageously, even with a high energy accelerator, by extracting pions at a relatively low energy between 100 MeV and 200 MeV. Although no experimental data appear to be available on the cross section for production of such low energy pions by multi-BeV protons, we can use experimental data on the production cross sections for higher energy pions together with an empirical formula for the pion energy spectrum to estimate the relevant differential cross sections for production of low energy pions.

All published experiments known to the authors which give production cross sections for pions of energy less than 1 BeV by incident protons of energy greater than 3 BeV are referred to in table 1, where the cross sections at the lowest pion energies of each experiment are listed. The column in table 1 entitled $(d^2 N/d\Omega dp)$ is the number of pions per steradian per BeV/c per circulating proton. These data

were obtained with the circulating internal beams at BNL and at CERN. The data in the column entitled $(d^2\sigma/d\Omega dp)$ were measured with an external proton beam. The data in the column entitled $(d^2\sigma/d\Omega dT)$ were calculated from the data on $(d^2\sigma/d\Omega dp)$ and $(d^2N/d\Omega dp)$. To obtain $(d^2\sigma/d\Omega dT)$ from $(d^2N/d\Omega dp)$ we use information on the ratio of interact-

ing protons to circulating protons⁹ and estimates of the total cross section for nuclear interaction of a proton. These data for a Be target are plotted in Figure 1. There are considerable unpublished data which we do not include, but which are generally consistent with the published data.

Table 1

EXPERIMENTAL POINTS AT LOWEST PION ENERGIES FOR DIFFERENT PROTON ENERGIES
(Laboratory coordinate system)

Proton Energy (BeV)	Target Element	Pion Energy (MeV)	θ	$\frac{d^2N}{d\Omega dp}$	Expt	$\frac{d^2\sigma}{d\Omega dp}$	Expt	$\frac{d^2\sigma}{d\Omega dT}$	Ref
				Pions per Circulating Proton/sr/(BeV/c)		$\mu\text{b/sr}/(\text{MeV/c})$ per Nucleus		$\mu\text{b/sr/MeV}$ per Nucleus	
30	Al	870 π^-	13°	0.2				136	6
30	Be	380 π^-	20°	0.09				30	6
30	Be	870 π^-	20°	0.1				32.3	6
30	Be	285 π^\pm	45°	0.07				24	5
30	Be	52 π^\pm	90°	0.045				21.2	5
30	Al	177 π^\pm	45°	0.07				52	5
20	Be	870 π^+	9°	0.65				210	6
18	H ₂	870 π^+	0°			28		28	7
18	Be	870 π^+	0°			240		242	7
18	H ₂	870 π^-	0°			26		26	7
18	Be	870 π^-	0°			229		231	7
18	Be	1850 π^\pm	5.7°			296		296	7
10	Be	870 π^-	9°	0.4				149	6
3	C	32 π^+	32°			32		65	8
3	C	105 π^+	32°			43		53	8
3	C	105 π^-	32°			30		37	8
3	C	193 π^-	32°			32		36	8
3	C	193 π^+	32°			47		52	8
3	C	285 π^+	32°			58		61	8
3	C	380 π^+	32°			47		49	8

The higher energy pion differential production cross section data including those shown in table 1 are fit approximately by the formula:⁷

$$\frac{d^2\sigma}{d\Omega dp} = \frac{n_\pi}{2\pi} \frac{4p^2}{\langle p_t \rangle^2 \langle p \rangle} \cdot \exp(-p/\langle p \rangle) \exp(-2p_t/\langle p_t \rangle) \quad (2)$$

which applies in the laboratory system of coordinates with p = pion momentum, p_t = transverse momentum of pion ($= p \sin \theta$ where θ = angle of emission of pion), $\langle p \rangle$ = mean momentum of pion, $\langle p_t \rangle$ = mean transverse momentum of pion, and n_π is the effective pion multiplicity. Typical values for the parameters which yield good fits to the experimental data are $\langle p \rangle = 2$ BeV/c and $\langle p_t \rangle = 350$ MeV/c. Note that

the shape of the pion energy spectrum is independent of the energy of the incident proton. However the mean pion multiplicity n_{π} increases as $E_0^{1/4}$ where E_0 is the primary proton energy. The peak of this spectrum occurs at a pion momentum p_m given by:

$$p_m = 2 \left[\frac{1}{\langle p \rangle} + \frac{2 \sin \theta}{\langle p_t \rangle} \right]^{-1}. \quad (3)$$

We use Eqn. (2) together with the experimental data to estimate the differential cross sections for low energy pion production in $p + \text{Be}$ collisions. Figure 2 shows the calculated differential cross sections at 5.7° for T_{π} from 50 MeV to 2000 MeV, where the calculations are normalized to an experimental point at $T_{\pi} = 1850$ MeV.⁷ The momentum spectra of positive and negative pions differ appreciably,⁷ but this difference appears small at low momenta and is very probably within the accuracy of our estimates. Note the sharp drop in the differential cross section at low energies; the decrease occurs essentially as p^2 in the low energy range. Since there is experimental evidence that the production of pions with low secondary momenta is more abundant at small angles than at 0° (7) and since it is more convenient experimentally to use a non-zero production angle, we shall use the cross section figures for 5.7° . There is also evidence⁷ that at small angles the cross section for production of pions with secondary momenta below 5 BeV/c is approaching a constant value in the laboratory system, independent of the primary momentum, so the primary proton energy is probably quite uncritical.

3. Production of Stopped Pions and Muons

For the production of stopped pions we must consider not only the differential cross section for pion production but also all the other factors in Eqn. (1). These include the intensity of the primary proton beam, the primary target thickness N , the optics of the beam transport system, pion decay (f_D), nuclear scattering of pions (f_A), and the range-energy relationship for pions (dT/dR). In addition, the effects of multiple Coulomb scattering of the pions is important.

We consider first the nuclear scattering of pions because it has a dominant effect on the choice of the pion extraction energy. The increase of straggling and transverse beam spread due to multiple Coulomb scattering with increase in the Z of the absorber indicates that a low Z absorber should be used, so we consider the use of a carbon absorber. In a nuclear scattering a pion can be absorbed in re-

actions such as $\pi^- + p \rightarrow n$ or $\pi^+ + n \rightarrow p$ with a nucleon in the nucleus, or it can also undergo an inelastic scattering which results in the breakup or excitation of the nucleus. We consider that either absorption or inelastic scattering will result in the loss of the pion from the stopping beam. Experimental data on the sum of the inelastic and absorption cross sections for pions on carbon as a function of pion energy are shown in Figure 3. The inelastic plus absorption cross sections are approximately equal for positive and negative pions.

Elastic nuclear scattering through a sufficiently large scattering angle can also cause the loss of the pion from the beam. However, the elastic cross section is peaked strongly forward due to diffraction scattering¹⁶ and does not contribute importantly to the attenuation of the pion beam.

The attenuation of the stopping pion beam is due principally to nuclear absorption and inelastic nuclear scattering. In computing f_A , it is a reasonable approximation to take the pion attenuation cross section for carbon σ_A as a constant equal to 300 mb (See Figure 3). Hence f_A is given by:

$$f_A = \exp \left[-N \int_0^T \frac{\sigma_A dT}{dT/dx} \right] = \exp(-3.8 \times 10^{-4} \times T^{1.7}) \quad (4)$$

where T is in MeV and $N = 10^{23}$ carbon atoms/cm³ (See Figure 4).

The fraction of pions which survive decay in flight, f_D , is given by:

$$f_D = 1 - \exp(-18.5 L/cp) \quad (5)$$

in which L = path length in meters (typical value is 10 m) and p is the laboratory momentum in MeV/c. In practice the principal part of the decay will occur in the magnet system used for extraction and focussing of the pions.

The range-energy relation for pions in carbon is given¹⁷ approximately by the equation:

$$R = a T^{1.7} \quad (6)$$

in which R = range in g/cm², T = pion kinetic energy in MeV, and $a = 0.011$ g/cm²-MeV. Hence the quantity dT/dR is given by

$$\frac{dT}{dR} = 53.5 T^{-0.7} \quad (7)$$

Multiple Coulomb scattering in the primary proton target or in the absorber leads to a lateral spread in the stopping

pion beam and to straggling. For a thick target the root mean square scattering angle tends toward a limiting value as the initial kinetic energy of the pion is increased, but the root mean square lateral spread continues to increase rapidly.² (It is about 1.1cm for $T_\pi = 100$ MeV, 2.7cm for 200 MeV and 4.2cm for 300 MeV). For many experiments the lateral spread in the beam which occurs for $T_\pi > 200$ MeV is excessive, and collimation and consequent reduction in intensity would be necessary. The percentage range straggling varies only slightly with T_π and amounts to about 3%, which in general will be smaller than the variation in mean range associated with the momentum range accepted by the magnet extraction system.¹⁸

Based on the above discussion the quantity $(dn_\pi/dR)/(INA\Omega)$ can be computed and is shown in Figure 5 as a function of T_π . In view of Figure 5 and the importance of multiple Coulomb scattering, we consider that $T_\pi = 150$ MeV is the most suitable energy for the production of a stopped pion beam.

With the above information we can compare the stopped pion yields from the BNL AGS - in particular we consider that the intensity of the AGS has been increased to 2×10^{13} protons/sec¹⁹ and from a low energy meson factory - in particular we consider the proton linear accelerator with 6×10^{15} protons/sec². The proton linear accelerator would be operated at about 450 MeV, where the differential cross section is about 60 $\mu\text{b}/\text{sr}/\text{MeV}/\text{nucleus}$ at 21° for π^+ mesons and 6 $\mu\text{b}/\text{sr}/\text{MeV}/\text{nucleus}$ for π^- mesons at the most suitable pion extraction energy of 100 MeV. For the AGS for $T_\pi = 150$ MeV the differential production cross section is about 30 $\mu\text{b}/\text{sr}-\text{MeV}$ per Be^9 nucleus. Hence the ratio of stopped pion yields from the linac and from the AGS external beam striking identical targets is given by:

$$\frac{\text{Linac yield}}{\text{AGS yield}} = \frac{(6 \times 10^{15}) \times (60) \times (0.60)}{(2 \times 10^{13}) \times (30) \times (0.48)} =$$

$$= \begin{cases} 750 & \text{for } \pi^+ \\ 75 & \text{for } \pi^- \end{cases}$$

Magnetic optics systems of the same efficiency are assumed for the two cases. The factor of 0.48 is the product $f_A \times f_D \times (dT/dR)$ and the factor of 0.60 is the similar one for the linac. The use of a much thicker target with the AGS external beam poses many difficulties associated with nuclear and Coulomb scattering of the low energy pions, the small pion production angle, and the optics of the magnetic extraction system.

We might also consider the use of a thin internal target with the improved AGS with multiple traversals. Although in principle the relative yield of the AGS should be improved by as much as a factor of 10 as compared to the external target, in practice this is not expected to be possible because a total dissipation of the beam energy on an internal target would lead to an unacceptable level of machine activation and radiation damage. Hence the yield ratio for the external target should be taken as the more realistic figure.

The ratios of the yields of stopped muons from the linac and from the AGS will be about the same as for stopped pions. The use of a muon channel at higher energies for the AGS would increase the muon flux from the channel but would not be useful for the production of stopped muons because of the lateral spread and straggling of the muon beam due to multiple Coulomb scattering.

Conclusion

In conclusion then, the use of the improved BNL AGS, which is the most favorable multi-BeV proton synchrotron for the production of stopped pions and muons, gives a yield some factor of 100 less than that of the proton linear accelerator meson factory. Furthermore, the background conditions near the AGS are probably more unfavorable than those near a low energy machine. Finally we might mention our belief that the political problem of using the most advanced high energy facility in the country for zero energy physics would be enormous.

References

1. F.T. Cole and A. Galonsky, p. 353 Proceedings of the International Conference on Sector-Focussed Cyclotrons and Meson Factories, CERN, 1963. Edited by F.T. Howard and N. Vogt-Nilsen.
2. "A Final Report on the Design of a Very High Intensity Proton Linear Accelerator as a Meson Factory at an Energy of 750 MeV." Yale Study of High Intensity Proton Accelerators Internal Report Y-12, October 1964.
3. D. Berley, "Low Energy Pion and Muon Fluxes at the AGS." Brookhaven National Laboratory - AADD Internal Report, April 1, 1964.
4. A. Citron, C. Delorme, F.J.M. Farley, L. Goldzahl, J. Heintze, E.G. Michaelis, M. Morpurgo and H. Øveras, Proceedings

of the Berkeley Conference on Instrumentation for High-Energy Physics, September 1960, p. 286; "The High Intensity Muon Beam with Low Pion Contamination at the CERN Synchro-Cyclotron," A. Citron, M. Morpurgo and H. Øveras, CERN 63-35, November 23, 1963.

5. V.L. Fitch, S.L. Meyer, and P.A. Piroué, Phys. Rev. 126, 1849 (1962).
6. W.F. Baker, R.L. Cool, E.W. Jenkins, T.F. Kycia, S.J. Lindenbaum, W.A. Love, D. Luers, J.A. Niederer, S. Ozaki, A.L. Read, J.J. Russell, and L.C.L. Yuan, Phys. Rev. Letters 7, 101 (1961).
7. D. Dekkers, J.A. Geibel, R. Mermod, G. Weber, T.R. Wilitts, K. Winter, B. Jordan, M. Vivargent, N.M. King, and E.J.N. Wilson, Phys. Rev. 137, B962 (1965).
8. A.C. Melissinos, T. Yamanouchi, G.G. Fazio, S.J. Lindenbaum, and L.C.L. Yuan, Phys. Rev. 128, 2373 (1962).
9. E.D. Courant, "Efficiency of Multiple Traversal Target." BNL Internal Report, EC-46, 1963.
10. D.V. Neagu and R.G. Saluvadze, Stul. Cercetari Fiz. (Roumania) 12, 39 (1961)
11. V.G. Ivanov, V.T. Osipenkov, N.I. Petrov, and V.A. Rusakov, Soviet Physics, JETP 10, 615 (1960).
12. A.E. Ignatenko, A.I. Mukhin, E.B. Ozerov, and B. Pontekorvo, Soviet Physics, JETP 31, 546 (1956).
13. V.G. Ivanov, V.T. Osipenkov, N.I. Petrov, and V.A. Rusakov, Soviet Physics, JETP 4, 922 (1957).
14. V.P. Dzhelepov, V.G. Ivanov, M.S. Kozadaev, V.T. Osipenkov, N.I. Petrov, and V.A. Rusakov, Soviet Physics, JETP 4, 864 (1957).
15. K.C. Wang, T.T. Wang, D.T. Ding, L.N. Dubrovskii, E.N. Kladnitskaia, and M.I. Solovev, Soviet Physics, JETP 8, 625 (1959).
16. R.M. Edelstein, W.F. Baker and J. Rainwater, Phys. Rev. 122, 252 (1961).
17. J.H. Atkinson and B.H. Willis, UCRL-2426(Rev.) Vol. II.
18. "Techniques of High Energy Physics," Edited by D.M. Ritson, Interscience, New York (1961).
19. "A Proposal for Increasing the Intensity of the Alternating Gradient Synchrotron at the Brookhaven National Laboratory," BNL 7956, May 1964.

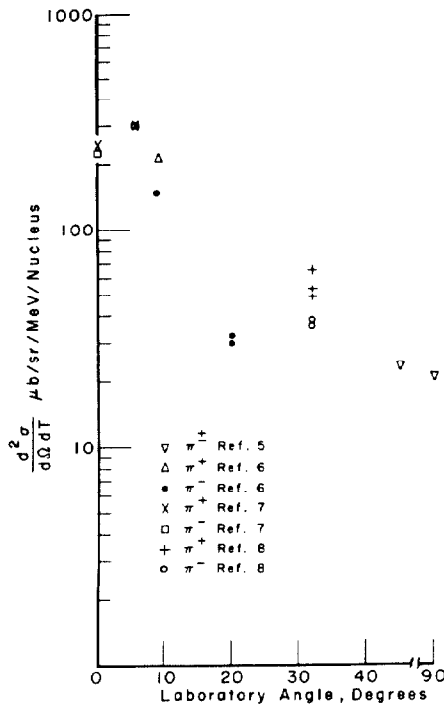


Fig. 1. Experimental differential cross sections, $d^2\sigma/d\Omega dT$, for pion production in the laboratory system by protons on Be^9 . Data are for pion kinetic energies less than 1 BeV with the exception of the point at 5.7° .

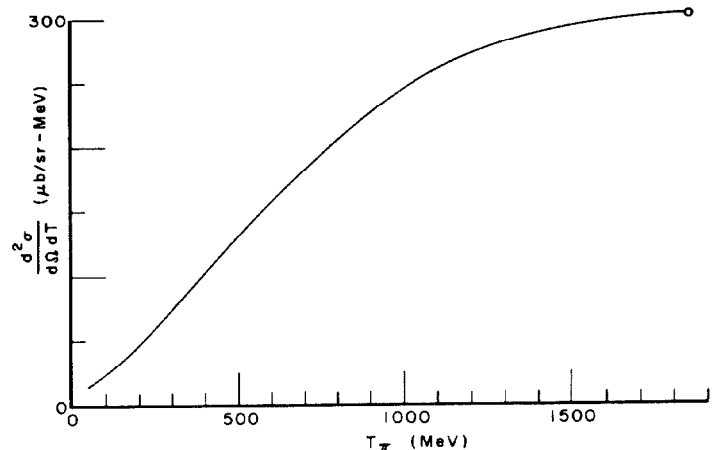


Fig. 2. Calculated differential cross sections $d^2\sigma/d\Omega dT$, vs. T in the laboratory system based on Equation (2). The calculated data are normalized to the indicated experimental point for protons of 18.8 BeV/c primary momentum on Be^9 and for $\theta = 5.7^\circ$.

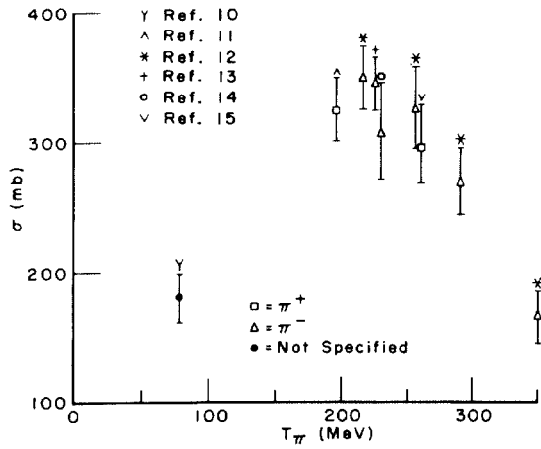


Fig. 3. Experimental data on the sum of the cross sections for absorption and inelastic scattering of pions on carbon.

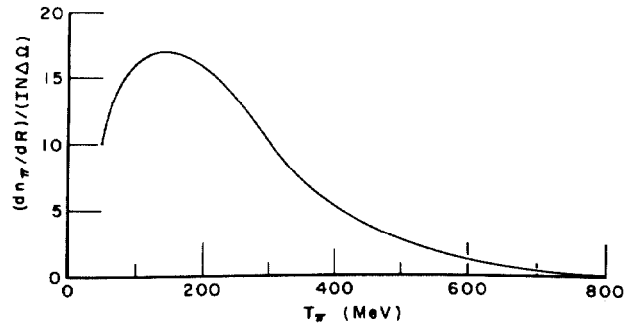


Fig. 5. The quantity $(dn_\pi/dR)/(NI\Delta\Omega)$ of Equation (1) vs. pion kinetic energy.

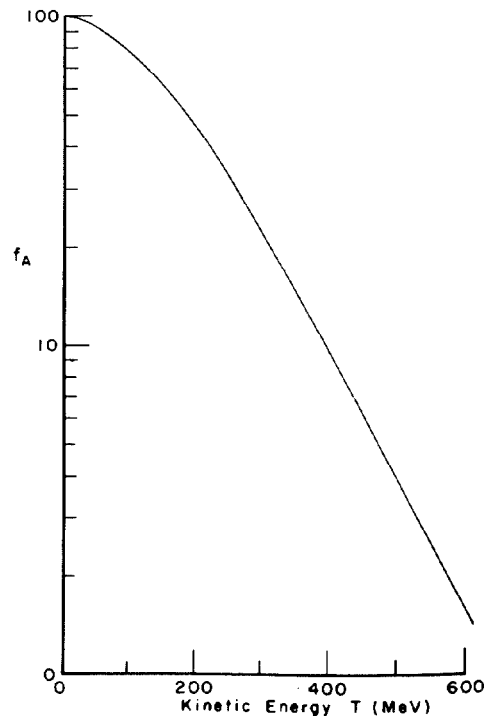


Fig. 4. Fraction, f_A , of stopping pions that survive and attenuating collision in a carbon absorber vs. initial pion kinetic energy.